Critical Growth of Cerebral Tissue in Organoids: Theory and Experiments

Egor I. Kiselev[1,2,*] Florian Pflug[1,3,*] and Arndt von Haeseler[1,4]
[1]Center for Integrative Bioinformatics Vienna (CIBIV), Max Perutz Laboratories, University of Vienna and Medical University of Vienna, Vienna Bio Center (VBC), 1030 Vienna, Austria
[2]Physics Department, Technion, 320003 Haifa, Israel
[3]Biological Complexity Unit, Okinawa Institute of Science and Technology Graduate University, Onna, Okinawa 904-0495, Japan
[4]Bioinformatics and Computational Biology, Faculty of Computer Science, University of Vienna, 1090 Vienna, Austria

(Received 12 June 2022; accepted 30 August 2023; published 24 October 2023)

We develop a Fokker-Planck theory of tissue growth with three types of cells (symmetrically dividing, asymmetrically dividing, and nondividing) as main agents to study the growth dynamics of human cerebral organoids. Fitting the theory to lineage tracing data obtained in next generation sequencing experiments, we show that the growth of cerebral organoids is a critical process. We derive analytical expressions describing the time evolution of clonal lineage sizes and show how power-law distributions arise in the limit of long times due to the vanishing of a characteristic growth scale. We discuss that the independence of critical growth on initial conditions could be biologically advantageous.

DOI: 10.1103/PhysRevLett.131.178402

Introduction.—The mechanisms of tissue growth and renewal are a core topic of stem-cell research [1,2]. In particular, the role of stochasticity in cell differentiation is discussed [3–8]. Single cell sequencing [9], combined with the labeling of cells with inheritable DNA sequences, enables large scale, quantitative studies of cell populations in biological tissues, where offspring populations can be traced back to their individual ancestral cells [10,11]. Such lineage tracing experiments have revealed that offspring numbers in mammalian cerebral tissue can vary by several orders of magnitude [6,12], which supports the hypothesis that stochasticity is an important property of cell proliferation and differentiation in the developing cerebral cortex.

This Letter presents a study of lineage tracing data obtained by sequencing 15 cerebral organoids at different stages of their development [12]. Cerebral organoids are highly controllable, self-organized *in vitro* models of the human cerebral cortex grown from stem cells. Organoids are unique because they model human tissues which cannot be studied *in vivo*. They have therefore become important biological tools to study neural development and brain diseases [13–15]. We take a physics point of view on the population dynamics of cell lineages in cerebral organoids, show that organoid growth is a critical process, and discuss the biological implications.

Model.—Our study begins with the observation that the numbers of descendants of an individual stem cell in the organoid (lineage sizes) are roughly distributed according to a $3/2$ power law. This behavior becomes more and more pronounced at late stages of the organoid development. To model the growth process mathematically, we build upon the theory of continuous state branching processes [16,17], pioneered by Feller [18]. These processes are known to lead to power-law distributed population sizes [19–21].

We thus introduce the *SAN model*. It consists of three agents: symmetrically dividing S-cells that represent stem cells, asymmetrically dividing A-cells, and nondividing N-cells (fully developed cells, e.g., neurons). S-cells undergo symmetric division ($S \to 2S$) at rate g_S, differentiation ($S \to A$) at rate g_A, and death ($S \to 0$) at rate g_0. A-cells have committed to a developmental trajectory and produce

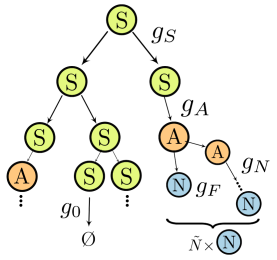

FIG. 1. The SAN model of dividing and differentiating cells. Stem cells (green, S) either divide at rate g_S ($S \to 2S$), differentiate at rate g_A ($S \to A$) or die at a rate g_0 ($S \to \emptyset$). Differentiated cells (orange, A) that committed to a developmental trajectory either divide asymmetrically ($A \to A + N$) at a rate g_A, or differentiate directly into nondividing N-cells (rate g_F). On average, each A-cell produces $\bar{N}$ N-cells until it loses the ability to divide. At criticality, the rates g_S (division) and g_A (differentiation) are equal.

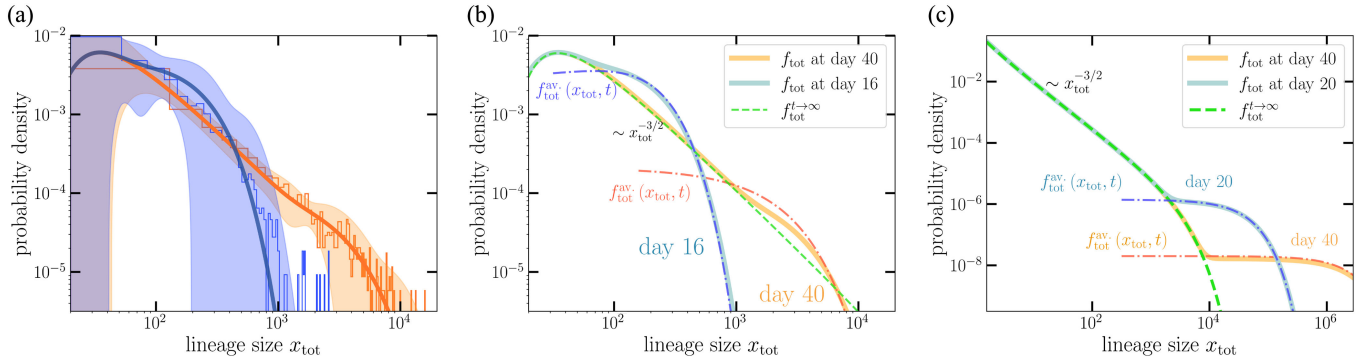

FIG. 2. (a) Histograms of lineage sizes of two organoids sequenced at $t = 16$ days (blue) and $t = 40$ days (orange) and the corresponding probability densities of the SAN model $f_{\rm tot}(x_{\rm tot}, t)$ (thick solid lines). Parameter values are given in Table I. Shaded areas indicate error margins. (b) Theoretical SAN model probability densities and the analytical approximations $f_{\rm tot}^{t\to\infty}(x_{\rm tot})$ (dashed, green line) and $f_{\rm tot}^{\rm av}(x_{\rm tot}, t)$ (dashed, dotted lines) of Eqs. (5) and (6) for the parameter estimates of Table I ($\alpha < 0$—subcritical regime). For $t \to \infty$ the distribution approaches the weakly truncated 3/2-power-law Lévy distribution $f_{\rm tot}^{t\to\infty}(x_{\rm tot})$ everywhere. (c) SAN model predictions for small $\alpha > 0$ (supercritical regime). $f_{\rm tot}(x_{\rm tot}, t)$ still approaches $f_{\rm tot}^{t\to\infty}(x_{\rm tot})$, except for very large lineage sizes, where the avalanche of active S-cell proliferation dominates. We used $\alpha = 0.2$, $\beta = 10$, $s_0 = 1$, and $N = 1$.

N-cells through asymmetric divisions ($A \to A + N$) at a rate g_N until the process is terminated by direct differentiation ($A \to N$) (rate g_F). The branching process of symmetric division and differentiation of S-cells with rates g_S and g_A are at the heart of the SAN model. Criticality is reached, when the two rates are equal: $g_S = g_A$. The model is illustrated in Fig. 1. We solve the SAN model analytically in the continuum limit and show how, at long times, 3/2-power-law distributions of cell populations asymptotically arise near criticality. Fitting the model predictions to the empirical data of Ref. [12], we show that cerebral organoid growth is indeed critical (see Fig. 2 and Table I).

In experiments, organoids are grown for 40 days. As we will demonstrate, our model can describe tissue growth as a dynamical process with a limited number of parameters—three rates and one initial condition.

Fokker-Planck description of lineage dynamics.—We start with a master equation for the SAN process. Individual populations of S, A, and N-cells are not accessible in experiments, since all descendants of a stem cell inherit the same lineage identifier. We therefore need to calculate the probability distribution of the total lineage size $x_{\rm tot} = s + a + n$. This calls for a slight simplification. We replace the processes $A \to A + N$ and $A \to N$ by the assumption that each A-cell produces $\bar{N} = 1 + g_N/g_F$ N-cells over the course of its existence (where the $+1$ stems from the final $A \to N$ conversion) (Fig. 1). Since the N-cell output per A-cell varies by multiple orders of magnitude less than the total offspring of an S-cell [22], this simplification does not affect the model's main predictions, making it analytically tractable. $\bar{N}$ is a fitting parameter in our theory. The total lineage size becomes $x_{\rm tot} = s + n$. The master equation for the probability distribution f of S- and N-cell numbers s, n at time t then reads as

$$\begin{aligned}\partial_t f(s,n,t) = {} & g_S(s-1)f(s-1,n,t) \\ & + g_A(s+1)f(s+1,n-\bar{N},t) \\ & + g_0(s+1)f(s+1,n,t) \\ & - (g_S s + g_A s + g_0 s)f(s,n,t). \end{aligned} \tag{1}$$

The right-hand side terms of Eq. (1) correspond to the different processes that the cells undergo: S-celll death at rate g_0, S-cell division at rate g_S, and differentiation into $\bar{N}$ N-cells at rate g_A. Focusing on large cell counts, we translate the discrete process of Eq. (1) into a continuous version given by the Fokker-Planck equation [23]:

$$\partial_t f(\mathbf{x}, t) = \mathcal{L} f(\mathbf{x}, t) \tag{2}$$

with the differential operator

$$\mathcal{L} = \left(-\alpha\partial_s + \frac{\beta}{2}\partial_s^2 - g_A\bar{N}\partial_s\partial_n - \bar{N}g_A\partial_n + \frac{g_A\bar{N}^2}{2}\partial_n^2 \right) s. \tag{3}$$

Here, $\mathbf{x} = (s, n)$ is a vector with continuous cell numbers as components, $\alpha = g_S - g_A - g_0$ and $\beta = g_S + g_A + g_0$.

Regimes of growth: Power laws and avalanches.—Next, we want to examine the implications of the Fokker-Planck Eq. (2) for the lineage sizes within a tissue sample. We solve Eq. (2) with the initial condition $f(\mathbf{x}, t = 0) = \delta(s - s_0)\delta(n)$. s_0 corresponds to the initial number of stem cells of a lineage—not necessarily unity, since stem cells proliferate at initial stages of organoid preparation, which are not considered here otherwise. Using the Fourier transform of Eqs. (2) and (3) with respect to $\mathbf{x}$ and the method of characteristics to solve the resulting first order partial differential equation (see the Supplemental

Material [24]), we find the characteristic function of $f(\mathbf{x},t)$, $\tilde{f}(\mathbf{q},t)=\int_{-\infty}^{\infty}e^{-i\mathbf{q}\cdot\mathbf{x}}f(\mathbf{x},t)$.

The distribution of total lineage sizes x_{tot} is given by an integral of $f(\mathbf{x},t)$ over all states with equal x_{tot}:

$$f_{\mathrm{tot}}(x_{\mathrm{tot}},t)=\int_0^{x_{\mathrm{tot}}}f(s,x_{\mathrm{tot}}-s,t)ds. \tag{4}$$

The presence of a critical point can be clearly seen from the expectation value of the stem-cell population: for finite α, $\langle s\rangle=s_0e^{\alpha t}$, whereas for the critical $\alpha=0$, $\langle s\rangle=s_0$. For $t\to\infty$, $f_{\mathrm{tot}}(x_{\mathrm{tot}},t)$ approaches a limiting distribution $f_{\mathrm{tot}}^{t\to\infty}(x_{\mathrm{tot}})$—a truncated 3/2-power-law Lévy distribution [25–27]:

$$f_{\mathrm{tot}}^{t\to\infty}(x_{\mathrm{tot}})\approx\frac{s_0\beta e^{-\frac{\alpha^2x_{\mathrm{tot}}}{\beta^2\bar{N}}}}{2\sqrt{2\pi}\bar{N}(x_{\mathrm{tot}}/\bar{N})^{3/2}}. \tag{5}$$

This formula holds for $\alpha\ll\beta$. For a more general expression see Eq. (S 28) in the Supplemental Material [24]. At criticality the distribution becomes a true 3/2 power law.

The way in which $f_{\mathrm{tot}}(x_{\mathrm{tot}},t)$ approaches the limit of Eq. (5) is very different for $\alpha>0$ and $\alpha<0$. For positive α and large enough lineage size $x_{\mathrm{tot}}>x_{\mathrm{tot}}^*\sim e^{\alpha t}$, there is a region where $f_{\mathrm{tot}}(x_{\mathrm{tot}},t)$ is not approximated by Eq. (5). This is the *avalanche region* illustrated in Fig. 2(c). Here, lineages have a high percentage of proliferating S-cells which are driving the system's growth. The lineage sizes are very large, but the probability of their occurrence is very small. For $x_{\mathrm{tot}}<x_{\mathrm{tot}}^*$ most lineages are fully differentiated and have stopped growing. In the avalanche regime, $f_{\mathrm{tot}}(x_{\mathrm{tot}},t)$ can be approximated by

$$f_{\mathrm{tot}}^{\mathrm{av}}(x_{\mathrm{tot}},t)\approx\frac{\sqrt{a}\exp\left(-\frac{a}{q_{\mathrm{tot}}^*}-\frac{x_{\mathrm{tot}}}{q_{\mathrm{tot}}^*\bar{N}}\right)}{q_{\mathrm{tot}}^*\sqrt{x_{\mathrm{tot}}\bar{N}}}I_1\left(2\sqrt{\frac{ax_{\mathrm{tot}}}{q_{\mathrm{tot}}^{*2}\bar{N}}}\right) \tag{6}$$

where $I_1(z)$ is the modified Bessel function of the first kind and $q_{\mathrm{tot}}^*(t)$ and $a(t)$ are defined in Eqs. (S 37) and (S 42) in the Supplemental Material [24].

For $\alpha<0$, we also find an avalanche region with an active S-cell population approximately described by Eq. (6) (even though the avalanche will stop eventually). As pointed out in the Supplemental Material [24], the approximation breaks down for $\alpha t>1$, but is still reasonable for the data at hand. This region is located at large x_{tot}, for which $f_{\mathrm{tot}}(x_{\mathrm{tot}},t)>f_{\mathrm{tot}}^{t\to\infty}(x_{\mathrm{tot}})$, followed by a rapid truncation at even larger x_{tot} [Fig. 2(b)]. In contrast to the behavior at $\alpha>0$, $f_{\mathrm{tot}}(x_{\mathrm{tot}},t)$ converges to $f_{\mathrm{tot}}^{t\to\infty}(x_{\mathrm{tot}})$ uniformly: the avalanches becomes less and less pronounced as $t\to\infty$, because the S-cells of all lineages eventually fully differentiate if $\alpha\le0$ [18]. Our analysis of the data shows that $\alpha\lesssim0$ holds in experiments (see Table I).

TABLE I. Parameters of the SAN model estimated from experimental data with 1 standard deviation error. α is the net growth rate of the stem-cell population, and β characterizes the stochasticity of the system. s_0 and $\bar{N}$ are the average initial number of stem cells and the average number of N-cells produced by each stem cell, respectively.

α (day^{-1})	-0.018 ± 0.004
β (day^{-1})	4 ± 1
s_0	9 ± 3
$\bar{N}$	2 ± 1

Dynamics and criticality in experiments.—The experimental data consist of lineage identifier counts for 15 organoids that were sequenced on days 16, 21, 25, 32, and 40—three copies for each day [12]. Accounting for statistical and readout errors, they can be related to lineage sizes [22]. Each organoid consists of $\sim10^4$ lineages, while total cell counts evolve from $\sim10^5$ at day 16 to $\sim10^6$ at day 40. The organoids grow undisturbed from day 11 onward, when they are not subjected to intrusive procedures anymore. Four parameters are determined from experimental data: α, β, s_0, and $\bar{N}$. The data at day 40 is very roughly distributed according to an $x^{-3/2}$ power law (see Fig. 2), indicating near critical growth with $\alpha\ll\beta$.

To determine the parameters precisely, we use the empirical characteristic function of the data

$$\tilde{f}_{\mathrm{exp}}(q_{\mathrm{tot}})=\sum_k e^{iq_{\mathrm{tot}}x_{\mathrm{tot}}^{(k)}}. \tag{7}$$

Here $x_{\mathrm{tot}}^{(i)}$ are the experimentally determined lineage sizes. The characteristic function of our model $\tilde{f}(q_{\mathrm{tot}},t)$ [Eq. (S 33)] is then least squares fitted to $\tilde{f}_{\mathrm{exp}}(q_{\mathrm{tot}})$. Moving the fitting procedure to Fourier space has several advantages: $\tilde{f}_{\mathrm{exp}}(q_{\mathrm{tot}})$ is less noisy than the empirical probability distribution, and no smoothing procedures such as kernel density estimates need to be used. Approximations needed when transforming $\tilde{f}(q_{\mathrm{tot}},t)$ to real space are avoided. Model fitting via the characteristic function has been considered, e.g., in Refs. [28,29]. Our estimates for the model parameters are shown in Table I. In Fig. 2(a) we show a comparison between the probability densities of the SAN model $f_{\mathrm{tot}}(x_{\mathrm{tot}},t)$ and binned histograms of the data at days 16 and 40. We used 500 bins for the data at day 40, and 80 bins for day 16. In the Supplemental Material [24], we show that the agreement is independent of bin size. Small lineages (<20 cells) were excluded since these lineages, with a high probability, died out at preparatory stages. $f_{\mathrm{tot}}(x_{\mathrm{tot}},t)$ is found using a fast Fourier transform of $\tilde{f}(q_{\mathrm{tot}},t)$.

The estimates of Table I show that organoid growth is indeed a critical process with $|\alpha|\ll\beta$. It also shows that even at day 40 the process is far from its $t\to\infty$ limit

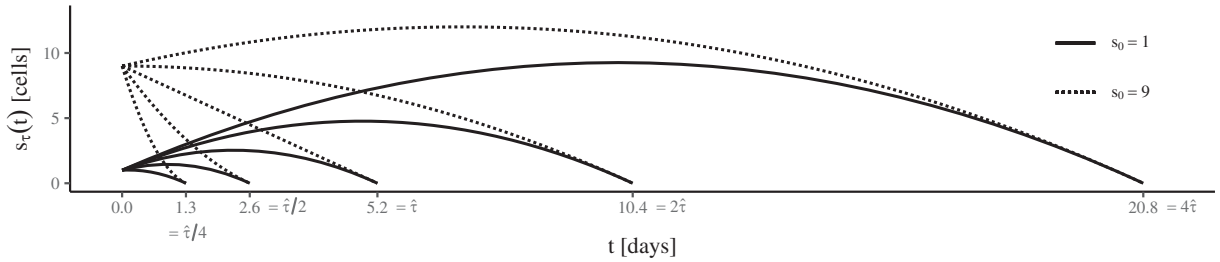

FIG. 3. Single lineage stem-cell populations for initial sizes $s_0 = 1$ (solid lines) and $s_0 = 9$ (dotted lines) and different extinction times τ [see Eq. (9)]. For large extinction times τ, the trajectories for $s_0 = 1$ and $s_0 = 9$ become equal for large times: In the critical state the population dynamics is dominated by stochasticity, and hence obtains a universal form independent of the initial conditions.

($\alpha t \approx 0.8$) and the organoids maintain an avalanchelike population of S-cells at large x_{tot}.

The *SAN model* is only a minimal model of biological reality and as such cannot account for the full spread of the experimental data. It does, for example, not account for the data at small x_{tot} (see Fig. 2). Many small lineages have died out in the early stages of the organoid development and are obviously not described by SAN dynamics. We assumed that all lineages consist of s_0 stem cells at day 11. This is only an average. While for large lineages the initial number of stem cells is unimportant since the growth is stochastic, it matters for lineages that differentiated quickly. Other neglected aspects are the time dependence of rates, and the non-Markovian nature of division and differentiation. Despite these caveats, the *SAN model* proves to be surprisingly robust and fits the experimental data well. In the Supplemental Material [24], Sec. D, we perform Kolmogorov-Smirnov (KS) tests on different intervals for the data at day 40. KS tests are a sensitive tool to test the power-law behavior of empirical data [30–32]. We find that the test produces high p-values (up to $p \approx 0.8$) in the region between $x_{\mathrm{tot}} \approx 200$ and $x_{\mathrm{tot}} \approx 2000$, where the power law is most pronounced.

Extinction trajectories.—We now turn to the influence of criticality on the dynamics of single lineages. We focus on $\alpha = 0$ and restrict ourselves to S-cells as the only dynamical component. Neglecting the dynamics of the n variable, we drop all but the first two terms in $\mathcal{L}$ in Eq. (3). The reduced Fokker-Planck equation is equivalent to the stochastic differential equation

$$ds = \sqrt{\beta s}\, dw(t). \tag{8}$$

$w(t)$ is the standard Brownian motion. It is known that any $s(t)$ described by Eq. (8), at some time τ, reaches $s(\tau) = 0$ [18], i.e., the S-cell population of the lineage goes extinct due to differentiation. Using the Onsager-Machlup formalism [33], we find the *extinction trajectory*

$$s_\tau(t) = s_0\left(1 - \frac{1}{\tau}\right)\left(1 + \left(\frac{\tau}{\hat{\tau}} - 1\right)\frac{t}{\tau}\right). \tag{9}$$

It describes the most probable path between $s(0) = s_0$ and $s(\tau) = 0$ (see Fig. 3). Here, $\hat{\tau} = 4s_0/\left(\sqrt{3}\beta\right)$. Details of the calculation are given in the Supplemental Material [24]. Equation (9) and Fig. 3 show that at criticality, the cells lose memory of the initial condition s_0, since for $\hat{\tau} \ll t < \tau$

$$s_\tau(t) \sim \sqrt{3}\beta t(1 - t/\tau)/4. \tag{10}$$

This is not the case for $\alpha \gtrless 0$.

Most importantly, since the lineage sizes are power-law distributed, an overwhelming majority of organoid cells will belong to a few very large lineages. For these lineages, $\tau \gg \hat{\tau}$ will hold, meaning that their development will be largely independent of the initial condition s_0 [Eq. (10)]. This is an essential feature of critical growth: it is independent of the initial conditions.

Discussion.—Finally, we discuss possible implications of critical tissue growth. Tuning itself to the critical point, the organoid maximizes the stochasticity of the growth process. We are not dealing with stochastic growth at a given rate. Instead, the characteristic timescale of growth vanishes ($\alpha = 0$), and growth is fully determined by the stochasticity of the process. This is in contrast to many other examples of organ growth and regeneration [34–36] where the growth process is arrested in a coordinated manner. In critical growth, the long term dynamics of large lineages, which make up most of the organoid, does not depend on initial conditions. Stochastic fluctuations have erased all memory of the lineage's initial size. This might hint at a biological advantage of the critical regime: the outcome of the growth process is less influenced by perturbations in its initial stages, when the tissue is most susceptible to disturbances.

Second, the critical nature of the process implies a mechanism balancing the rates of division and differentiation of stem cells. Such balancing mechanisms are known from homeostatic stem-cell renewal [37]. One distinguishes between mechanisms based on asymmetric division (only one daughter cell is a stem cell while the other differentiates) and population asymmetry (the rates of stem-cell loss and division are balanced on the population level). The first strategy cannot produce critical lineage

dynamics because it is strictly deterministic. On the population level, stem-cell niches are a well-known regulatory mechanism for homeostatic tissues [7,38,39] found in intestinal crypts [38] and the adult human brain [40]. The available niche space limits the number of possible divisions. For growing tissues, the competition for a scarce resource, e.g., space or nutrients, can provide a feedback loop that limits the stem cells' ability for division at the population level. Such a feedback loop is often encountered in models of self-organized criticality (SOC) [19], where the event probabilities are balanced and tuned to the critical point, e.g., by energy conservation. For cerebral tissue, the currently available data give no clues to the nature of the balancing mechanism. The search, however, could inspire future experimental research. Recent advances in lineage tracing allow one to study the spatial distribution of lineages in cerebral organoids using light-sheet microscopy and spatial transcriptome sequencing [41]. Inferring the spatial dynamics of the growth process could help to identify the mechanism behind organoid SOC. Quantitative lineage tracing experiments with other organoid types such as intestinal [42,43], retinal [44,45], or cardiac organoids [46,47] could reveal whether critical growth is specific to cerebral tissue, or whether it is a more general organizing principle.

We thank C. Esk, N. Goldenfeld, S. Haendeler, B. Jeevanesan, J. F. Karcher, and D. Lindenhofer for inspiring discussions. This project has received funding from the European Union's Framework Programme for Research and Innovation Horizon 2020 (20142020) under the Marie Curie Skłodowska Grant Agreement No. 847548 (A. vH., E. K.), and from a Special Research Programme (SFB) of the Austrian Science Fund (FWF), Project No. F78 P11 (A. vH., F. P.).

*E. K. and F. P. contributed equally to this work.

[1] Lemonia Chatzeli and Benjamin D. Simons, Tracing the dynamics of stem cell fate, Cold Spring Harbor Perspect. Biol. **12**, a036202 (2020).

[2] Benjamin D. Simons and Hans Clevers, Strategies for homeostatic stem cell self-renewal in adult tissues, Cell **145**, 851 (2011).

[3] Yang Lin, Jiajun Yang, Zhongfu Shen, Jian Ma, Benjamin D. Simons, and Song-Hai Shi, Behavior and lineage progression of neural progenitors in the mammalian cortex, Curr. Opin. Neurobiol. **66**, 144 (2021).

[4] Christoph Zechner, Elisa Nerli, and Caren Norden, Stochasticity and determinism in cell fate decisions, Development **147**, dev181495 (2020).

[5] Esther Klingler and Denis Jabaudon, Cortical development: Do progenitors play dice?, eLife **9**, e54042 (2020).

[6] Alfredo Llorca, Gabriele Ciceri, Robert Beattie, Fong Kuan Wong, Giovanni Diana, Eleni Serafeimidou-Pouliou, Marian Fernandez-Otero, Carmen Streicher, Sebastian J. Arnold, Martin Meyer *et al.*, A stochastic framework of neurogenesis underlies the assembly of neocortical cytoarchitecture, eLife **8**, e51381 (2019).

[7] Bernat Corominas-Murtra, Colinda L. G. J. Scheele, Kasumi Kishi, Saskia I. J. Ellenbroek, Benjamin D. Simons, Jacco Van Rheenen, and Edouard Hannezo, Stem cell lineage survival as a noisy competition for niche access, Proc. Natl. Acad. Sci. U.S.A. **117**, 16969 (2020).

[8] Quinton Smith, Evgeny Stukalin, Sravanti Kusuma, Sharon Gerecht, and Sean X. Sun, Stochasticity and spatial interaction govern stem cell differentiation dynamics, Sci. Rep. **5**, 1 (2015).

[9] Yukie Kashima, Yoshitaka Sakamoto, Keiya Kaneko, Masahide Seki, Yutaka Suzuki, and Ayako Suzuki, Single-cell sequencing techniques from individual to multiomics analyses, Exp. Mol. Med. **52**, 1419 (2020).

[10] Daniel E. Wagner and Allon M. Klein, Lineage tracing meets single-cell omics: Opportunities and challenges, Nat. Rev. Genet. **21**, 410 (2020).

[11] Lennart Kester and Alexander van Oudenaarden, Single-cell transcriptomics meets lineage tracing, Cell Stem Cell **23**, 166 (2018).

[12] Christopher Esk, Dominik Lindenhofer, Simon Haendeler, Roelof A. Wester, Florian Pflug, Benoit Schroeder, Joshua A. Bagley, Ulrich Elling, Johannes Zuber, Arndt von Haeseler *et al.*, A human tissue screen identifies a regulator of ER secretion as a brain-size determinant, Science **370**, 935 (2020).

[13] Madeline A. Lancaster, Magdalena Renner, Carol-Anne Martin, Daniel Wenzel, Louise S. Bicknell, Matthew E. Hurles, Tessa Homfray, Josef M. Penninger, Andrew P. Jackson, and Juergen A. Knoblich, Cerebral organoids model human brain development and microcephaly, Nature (London) **501**, 373 (2013).

[14] Madeline A. Lancaster, Nina S. Corsini, Simone Wolfinger, E. Hilary Gustafson, Alex W. Phillips, Thomas R. Burkard, Tomoki Otani, Frederick J. Livesey, and Juergen A. Knoblich, Guided self-organization and cortical plate formation in human brain organoids, Nat. Biotechnol. **35**, 659 (2017).

[15] Jihoon Kim, Bon-Kyoung Koo, and Juergen A. Knoblich, Human organoids: Model systems for human biology and medicine, Nat. Rev. Mol. Cell Biol. **21**, 571 (2020).

[16] William Feller, Two singular diffusion problems, Ann. Math. **54**, 173 (1951).

[17] John Lamperti, The limit of a sequence of branching processes, Z. Wahrsch. Verw. Geb. **7**, 271 (1967).

[18] Willy Feller, Die Grundlagen der Volterraschen Theorie des Kampfes ums Dasein in wahrscheinlichkeitstheoretischer Behandlung, Acta Biotheoretica **5**, 11 (1939).

[19] Stefano Zapperi, Kent Bækgaard Lauritsen, and H. Eugene Stanley, Self-Organized Branching Processes: Mean-Field Theory for Avalanches, Phys. Rev. Lett. **75**, 4071 (1995).

[20] Mikko J. Alava and Kent Bækgaard Lauritsen, Branching processes, in *Computational Complexity: Theory, Techniques, and Applications* (Springer, New York, 2012), pp. 285–297, 10.1007/978-1-4614-1800-9_19.

[21] Serena di Santo, Pablo Villegas, Raffaella Burioni, and Miguel A. Muñoz, Simple unified view of branching

process statistics: Random walks in balanced logarithmic potentials, Phys. Rev. E **95**, 032115 (2017).
[22] Florian G. Pflug, Simon Haendeler, Christopher Esk, Dominik Lindenhofer, Jürgen A. Knoblich, and Arndt von Haeseler, Neutral competition within a long-lived population of symmetrically dividing cells shapes the clonal composition of cerebral organoids, bioRxiv (2021), 10.1101/2021.10.06.463206.
[23] N. G. van Kampen, *Stochastic Processes in Physics and Chemistry* (North Holland, Amsterdam, 2007), iSBN: 978-0444529657.
[24] See Supplemental Material at http://link.aps.org/supplemental/10.1103/PhysRevLett.131.178402 for detailed derivations of the analytical results.
[25] Constantino Tsallis, Lévy distributions, Phys. World **10**, 42 (1997).
[26] B. V. Gnedenko and A. N. Kolmogorov, Limit distributions for sums of independent random variables, Am. J. Math. **105** (1954).
[27] Jean-Philippe Bouchaud and Antoine Georges, Anomalous diffusion in disordered media: Statistical mechanisms, models and physical applications, Phys. Rep. **195**, 127 (1990).
[28] Jun Yu, Empirical characteristic function estimation and its applications, Econom. Rev. **23**, 93 (2004).
[29] Ngai Hang Chan, Song Xi Chen, Liang Peng, and Cindy L. Yu, Empirical likelihood methods based on characteristic functions with applications to lévy processes, J. Am. Stat. Assoc. **104**, 1621 (2009).
[30] Aaron Clauset, Cosma Rohilla Shalizi, and Mark E. J. Newman, Power-law distributions in empirical data, SIAM Rev. **51**, 661 (2009).
[31] Jonathan Touboul and Alain Destexhe, Can power-law scaling and neuronal avalanches arise from stochastic dynamics?, PLoS One **5**, e8982 (2010).
[32] Jonathan Touboul and Alain Destexhe, Power-law statistics and universal scaling in the absence of criticality, Phys. Rev. E **95**, 012413 (2017).
[33] Detlef Dürr and Alexander Bach, The Onsager-Machlup function as Lagrangian for the most probable path of a diffusion process, Commun. Math. Phys. **60**, 153 (1978).
[34] Nelson Fausto, Liver regeneration, J. Hepatol. **32**, 19 (2000).
[35] Qi Zeng and Wanjin Hong, The emerging role of the hippo pathway in cell contact inhibition, organ size control, and cancer development in mammals, Cancer Cell **13**, 188 (2008).
[36] Anna P. Ainslie, John Robert Davis, John J. Williamson, Ana Ferreira, Alejandro Torres-Sanchez, Andreas Hoppe, Federica Mangione, Matthew B. Smith, Enrique Martin-Blanco, Guillaume Salbreux *et al.*, ECM remodeling and spatial cell cycle coordination determine tissue growth kinetics, bioRxiv (2020), 10.1101/2020.11.10.376129.
[37] Benjamin D. Simons and Hans Clevers, Strategies for homeostatic stem cell self-renewal in adult tissues, Cell **145**, 851 (2011).
[38] Kateri A. Moore and Ihor R. Lemischka, Stem cells and their niches, Science **311**, 1880 (2006).
[39] Ruihe Lin and Lorraine Iacovitti, Classic and novel stem cell niches in brain homeostasis and repair, Brain Res. **1628**, 327 (2015).
[40] Arturo Alvarez-Buylla and Daniel A. Lim, For the long run: Maintaining germinal niches in the adult brain, Neuron **41**, 683 (2004).
[41] Zhisong He, Ashley Maynard, Akanksha Jain, Tobias Gerber, Rebecca Petri, Hsiu-Chuan Lin, Malgorzata Santel, Kevin Ly, Jean-Samuel Dupré, Leila Sidow *et al.*, Lineage recording in human cerebral organoids, Nat. Methods **19**, 90 (2022).
[42] Hamish C. K. Angus, A. Grant Butt, Michael Schultz, and Roslyn A. Kemp, Intestinal organoids as a tool for inflammatory bowel disease research, Front. Med. **6**, 334 (2020).
[43] Shoichi Date and Toshiro Sato, Mini-gut organoids: Reconstitution of the stem cell niche, Annu. Rev. Cell Dev. Biol. **31**, 269 (2015).
[44] Manuela Völkner, Marlen Zschätzsch, Maria Rostovskaya, Rupert W. Overall, Volker Busskamp, Konstantinos Anastassiadis, and Mike O. Karl, Retinal organoids from pluripotent stem cells efficiently recapitulate retinogenesis, Stem Cell Rep. **6**, 525 (2016).
[45] Giorgia Quadrato, Tuan Nguyen, Evan Z. Macosko, John L. Sherwood, Sung Min Yang, Daniel R. Berger, Natalie Maria, Jorg Scholvin, Melissa Goldman, Justin P. Kinney *et al.*, Cell diversity and network dynamics in photosensitive human brain organoids, Nature (London) **545**, 48 (2017).
[46] Bramasta Nugraha, Michele F. Buono, Lisa von Boehmer, Simon P. Hoerstrup, and Maximilian Y. Emmert, Human cardiac organoids for disease modeling, Clinical pharmacology and therapeutics **105**, 79 (2019).
[47] Plansky Hoang, Jason Wang, Bruce R. Conklin, Kevin E. Healy, and Zhen Ma, Generation of spatial-patterned early-developing cardiac organoids using human pluripotent stem cells, Nat. Protocols **13**, 723 (2018).